sequences to the transcriptional machinery (*2*, *5*). At the same time, hyperacetylation within gene bodies is a prerequisite for MSL complex binding to the transcribed regions of X-linked genes (*1*). Restricting the MSL complex to these sites may prevent the physical obstruction of promoters in males and thereby help to balance the transcriptional output between sexes.

References and Notes

1. T. Conrad, A. Akhtar, *Nat. Rev. Genet.* **13**, 123 (2012).
2. M. E. Gelbart, E. Larschan, S. Peng, P. J. Park, M. I. Kuroda, *Nat. Struct. Mol. Biol.* **16**, 825 (2009).
3. F. N. Hamada, P. J. Park, P. R. Gordadze, M. I. Kuroda, *Genes Dev.* **19**, 2289 (2005).
4. T. Straub, G. D. Gilfillan, V. K. Maier, P. B. Becker, *Genes Dev.* **19**, 2284 (2005).
5. O. Bell *et al.*, *Nat. Struct. Mol. Biol.* **17**, 894 (2010).
6. S. W. Park, H. Oh, Y. R. Lin, Y. Park, *Biochem. Biophys. Res. Commun.* **399**, 227 (2010).
7. J. C. Lucchesi, *Curr. Opin. Genet. Dev.* **8**, 179 (1998).
8. E. Larschan *et al.*, *Nature* **471**, 115 (2011).
9. T. Conrad *et al.*, *Dev. Cell* **22**, 610 (2012).
10. J. Kind *et al.*, *Cell* **133**, 813 (2008).
11. J. Zeitlinger *et al.*, *Nat. Genet.* **39**, 1512 (2007).
12. G. W. Muse *et al.*, *Nat. Genet.* **39**, 1507 (2007).
13. S. Nechaev *et al.*, *Science* **327**, 335 (2010).
14. A. M. Johansson, P. Stenberg, A. Allgardsson, J. Larsson, *Mol. Cell. Biol.* **32**, 2121 (2012).
15. J. H. Malone *et al.*, *Genome Biol.* **13**, r28 (2012).
16. C. Laverty, F. Li, E. J. Belikoff, M. J. Scott, *PLoS ONE* **6**, e20455 (2011).

Acknowledgments: We thank K. Adelman and J. Lis for kindly providing Rpb3 antibodies, the European Molecular Biology Laboratory (EMBL) GeneCore facility and I. De la Rosa for Illumina sequencing services, and the members of our groups for critical reading of the manuscript and helpful discussions. Supported by the European Union–funded EpiGeneSys (N.M.L. and A.A.); EMBL, Okinawa Institute of Science and Technology, and Cancer Research UK (N.M.L.); the EMBL Ph.D. program (T.C. and F.M.G.C.); and the European Science Foundation Exchange Grant program (J.M.V.). The Pol II ChIP-seq data are available in ArrayExpress under accession no. E-MTAB-1112.

Supplementary Materials

www.sciencemag.org/cgi/content/full/science.1221428/DC1
Materials and Methods
Figs. S1 to S10
Tables S1 to S3
References (*17*–*25*)

5 March 2012; accepted 4 June 2012
Published online 19 July 2012;
10.1126/science.1221428

Fate-Restricted Neural Progenitors in the Mammalian Cerebral Cortex

Santos J. Franco, Cristina Gil-Sanz,* Isabel Martinez-Garay,*† Ana Espinosa, Sarah R. Harkins-Perry, Cynthia Ramos, Ulrich Müller‡

During development of the mammalian cerebral cortex, radial glial cells (RGCs) generate layer-specific subtypes of excitatory neurons in a defined temporal sequence, in which lower-layer neurons are formed before upper-layer neurons. It has been proposed that neuronal subtype fate is determined by birthdate through progressive restriction of the neurogenic potential of a common RGC progenitor. Here, we demonstrate that the murine cerebral cortex contains RGC sublineages with distinct fate potentials. Using in vivo genetic fate mapping and in vitro clonal analysis, we identified an RGC lineage that is intrinsically specified to generate only upper-layer neurons, independently of niche and birthdate. Because upper cortical layers were expanded during primate evolution, amplification of this RGC pool may have facilitated human brain evolution.

The mammalian cerebral cortex consists of six major layers that each contain specific subtypes of neurons characterized by distinct projection patterns and gene expression profiles (*1*). These layer-specific classes of cortical excitatory neurons are derived from radial glial cells (RGCs) in sequential order, with neurons destined for lower layers being generated first, followed by upper-layer neurons and, finally, cortical astrocytes (*1*). This relationship between birthdate and laminar fate of neurons in the cerebral cortex has been documented for more than 50 years, although it has remained unclear whether cell fate is determined directly by birthdate (*2*) or if the two are linked more indirectly rather than causally (*3*).

RGCs divide asymmetrically in the cortical ventricular zone to self-renew and generate neurons directly or, more commonly, indirectly via intermediate progenitor cells that divide symmetrically in the ventricular and subventricular zones (*4*). The transcription factor Cux2 is expressed specifically in neurons in upper layers II to IV in the mature cortex (Fig. 1A), but also in intermediate progenitors in the developing subventricular zone (*5*, *6*), suggesting that upper- versus lower-layer fate might be determined before neuronal differentiation. We found that Cux2 mRNA is also expressed in the ventricular zone in a salt-and-pepper manner (Fig. 1B and fig. S1, A to D), indicating that some RGCs may be committed to generate upper-layer neurons. To establish the identity of ventricular zone $Cux2^+$ cells and to determine their lineage potential, we employed genetic fate mapping using a mouse strain expressing Cre recombinase from the *Cux2* locus (*7*). Crossing the *Cux2-Cre* driver line to reporter mouse lines led to recombination primarily in upper-layer neurons in the mature cortex, with 76% of recombined cells occupying layers II to IV (Fig. 1C and fig. S1, E to H). Only 17 and 7% of recombined cells were found in lower layers V and VI, respectively (Fig. 1C and fig. S1, E to H), and most of these were $Satb2^+$ excitatory neurons (74%) (fig. S1, I and J), which form callosal projections similar to layer II and III neurons (*8*, *9*). The remainder were $Gad65/67^+$ interneurons (26%) (fig. S1, I and J) derived from the ganglionic eminences, in agreement with previous observations (*6*). Furthermore, in the developing cortex we identified clonal columns of recombined cells in the ventricular zone (Fig. 1D), resembling the pattern of endogenous Cux2 mRNA expression. The majority of recombined cells in the ventricular zone expressed the RGC markers Pax6 (Fig. 1E) and nestin (Fig. 1F), but not the intermediate progenitor marker Tbr2 (Fig. 1G). Recombined cells divided at the ventricular surface (Fig. 1, H and I), maintained apical and basal processes, and underwent interkinetic nuclear migration (Fig. 1I), all hallmarks of ventricular zone RGCs. These results suggest that a subset of RGCs are restricted in their lineage potential.

To further analyze the relationship between $Cux2^+$ RGCs and their offspring, we introduced a Cre reporter plasmid into RGCs in *Cux2-Cre* embryos by in utero electroporation. In this FLEx (FLip-Excision) technology–based reporter plasmid (*10*), Cre recombination switches expression from tdTomato fluorescent protein to green fluorescent protein (GFP), thereby permitting differential fluorescent labeling of $Cux2^+$ and $Cux2^-$ RGCs and their offspring (Fig. 2A). Electroporation of the reporter at embryonic day (E) 12.5 and analysis at E13.5 demonstrated that a subset of electroporated RGCs had recombined the reporter and turned on GFP (Fig. 2B), even though at this early time point the tdTomato signal remained because of protein perdurance. At postnatal day (P) 10, 83% of neurons with recombined reporters (GFP^+) had settled in upper layers II to IV (Fig. 2, C and D), whereas only 7% of the neurons with nonrecombined reporters ($tdTom^+GFP^-$) were located in upper layers (Fig. 2, C and D). These results suggest that the $Cux2^+$ progenitors constitute a lineage largely fated to become upper-layer neurons with a small contribution to lower layers, whereas the $Cux2^-$ lineage primarily generates lower-layer neurons.

To facilitate temporal fate mapping of the $Cux2^+$ lineage, we generated a mouse line in which the tamoxifen-inducible *CreERT2* (*11*) gene is knocked into the endogenous *Cux2* locus (fig. S2, A to C). By crossing *Cux2-CreERT2* mice with a Cre-reporter strain and inducing recombination

Dorris Neuroscience Center and Department of Cell Biology, The Scripps Research Institute, 10550 North Torrey Pines Road, La Jolla, CA 92037, USA.

*These authors contributed equally to this work and are listed alphabetically.

†Present address: Department of Physiology, Anatomy, and Genetics, University of Oxford, Oxford OX1 3QX, UK.

‡To whom correspondence should be addressed. E-mail: umueller@scripps.edu

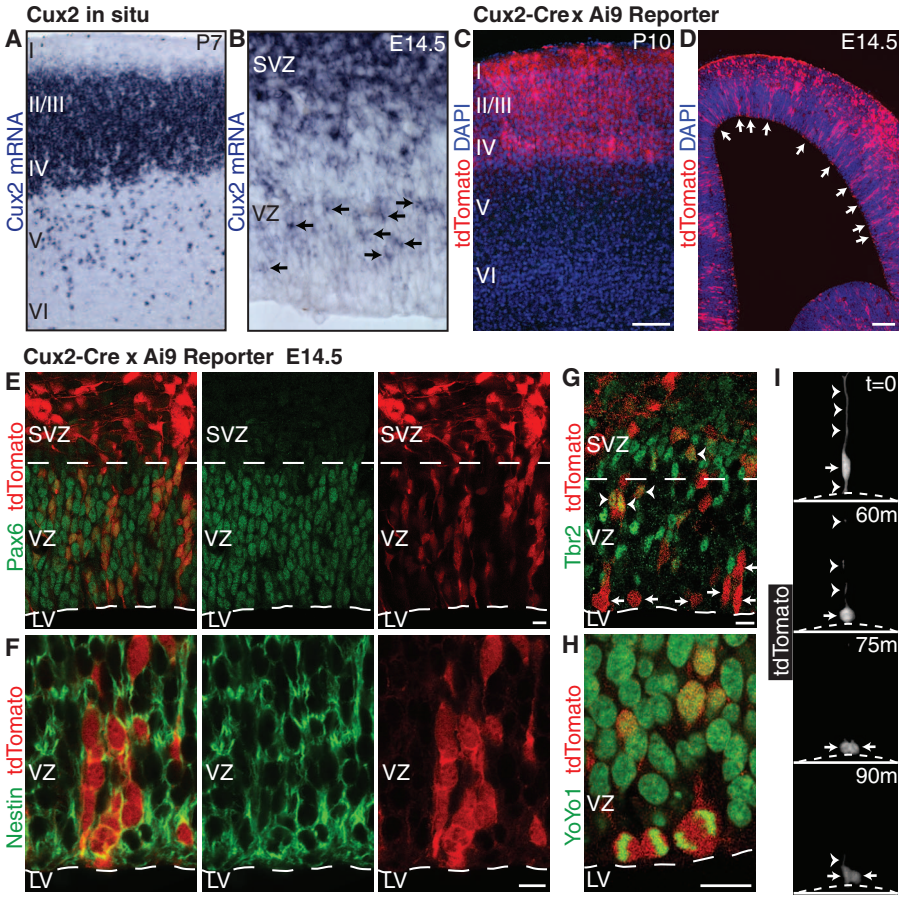

Fig. 1. Expression of Cux2 in a subset of RGCs suggests multiple progenitor types. (**A** and **B**) In situ hybridization shows Cux2 mRNA at P7 (A) and E14.5 (B). Arrows indicate expression in a subset of ventricular zone cells. (**C** and **D**) Cumulative fate mapping of the Cux2 lineage in *Cux2-Cre;Ai9* mice at P10 (C) and E14.5 (D). Arrows indicate recombination in a subset of ventricular zone cells. (**E** and **F**) Recombination in Pax6$^+$ (E) and nestin$^+$ (F) RGCs. (**G**) Recombination in Tbr2$^+$ intermediate progenitors (arrowheads) and Tbr2$^-$ RGCs (arrows) in the ventricular zone. (**H**) Recombined mitotic cells dividing at the ventricular surface. (**I**) Live imaging of a slice culture from a *Cux2-Cre;Ai9* embryo showing a recombined RGC (arrow) undergoing interkinetic nuclear migration and dividing at the ventricular surface (dotted line). Arrowheads, apical and basal radial processes. LV, lateral ventricle; SVZ, subventricular zone; VZ, ventricular zone. Scale bars, 100 μm [(C) and (D)] and 10 μm [(E) to (H)].

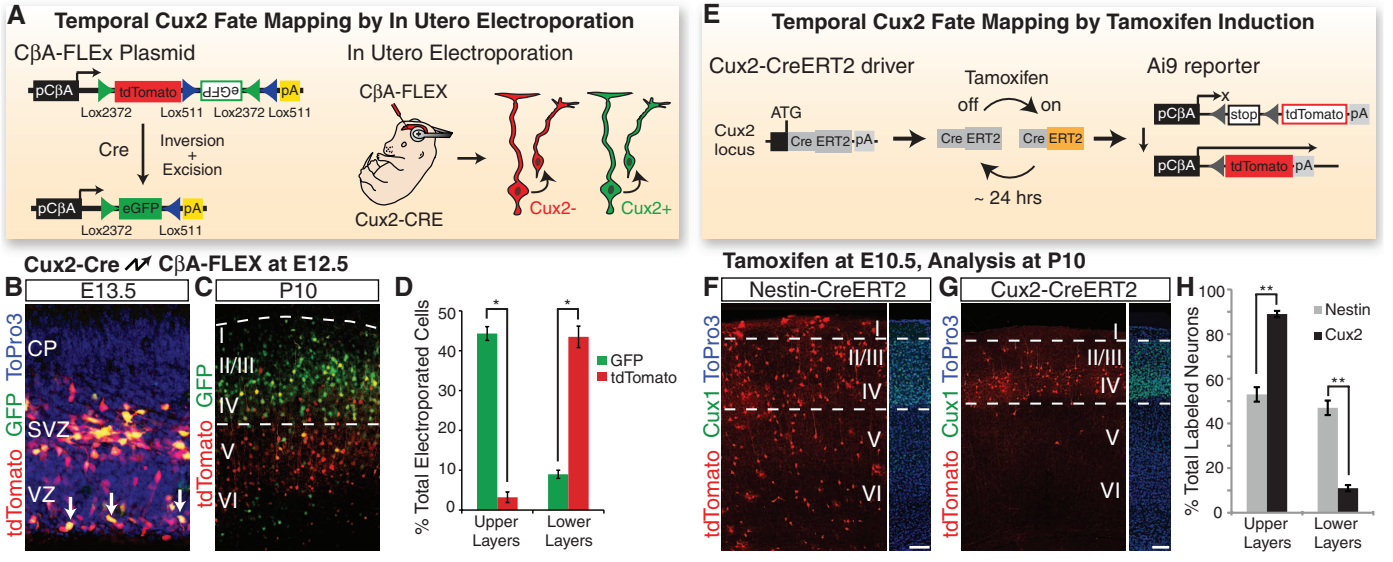

Fig. 2. RGCs of the Cux2 lineage are fated to generate upper-layer neurons. (**A**) Temporal fate mapping by in utero electroporation. Upon in utero electroporation into *Cux2-Cre* embryos, CβA-FLEx drives differential expression of tdTomato and enhanced GFP (eGFP) in Cux2$^-$ and Cux2$^+$ cells, respectively. (**B**) Electroporation of CβA-FLEx at E12.5, analysis at E13.5. Arrows identify cells in the ventricular zone that have recombined the plasmid. (**C**) Electroporation at E12.5, analysis at P10. (**D**) Percentage (±SEM) of electroporated GFP$^+$ and tdTomato$^+$ neurons in upper versus lower layers at P10. *$P < 0.0005$. (**E**) Temporal fate mapping by tamoxifen induction. *Cux2-CreERT2* mice allow temporary activation of CreERT2 in the Cux2$^+$ lineage within 6 to 24 hours after tamoxifen injection. CreERT2 activates the *Ai9* reporter to allow permanent tdTomato labeling during this window, but not before or after. (**F**) E10.5 induction, P10 analysis of a *Nestin-CreERT2* line, which drives recombination in Cux2$^+$ and Cux2$^-$ RGCs. Dotted lines frame Cux1 expression in upper layers. (**G**) E10.5 induction, P10 analysis of the *Cux2-CreERT2* line. (**H**) Percentage (±SEM) of recombined neurons in upper versus lower layers for each driver. *$P < 1 \times 10^{-10}$. CP, cortical plate. Scale bars, 100 μm.

with a single injection of tamoxifen (Fig. 2E), we can label the Cux2$^+$ lineage within a narrow ~24-hour window (*12*, *13*). Because most cortical cells are RGCs at E10.5, we injected tamoxifen at this time point to permanently label Cux2$^+$ RGCs between E10.5 and E11.5, but not before or afterward. We performed the same experiments with *Nestin-CreERT2* mice (*14*), which express tamoxifen-inducible Cre in all RGCs (fig. S2, D and E). Whereas the *Nestin-CreERT2* line labeled neurons that contributed to all cortical layers (Fig. 2, F and H), as well as astrocytes and oligodendrocytes (fig. S2, F and G), the *Cux2-CreERT2* line labeled predominantly neurons in upper layers (Fig. 2, G and H). Thus, Cux2$^+$ RGCs are fated to generate upper-layer neurons even at the earliest stages of cortical neurogenesis. Cux2$^-$ RGCs are likely the proposed bipotent neuroglial progenitors (*15*), or are perhaps further subdivided into lineage-restricted subtypes.

Lower-layer neurons are largely born before upper-layer neurons, although there is some degree of overlap in the birthdates of different neuronal subtypes (*16*). Because Cux2$^+$ upper-layer progenitors and Cux2$^-$ lower-layer progenitors coexist at the earliest stages of cortical development (fig. S3), we reasoned that during lower-layer neurogenesis, Cux2$^+$ RGCs might show a greater propensity to proliferate to expand the RGC pool, whereas Cux2$^-$ RGCs might preferentially generate neurons. In support of this idea, the percentage of Cux2$^+$ RGCs increased over time, whereas the percentage of Cux2$^-$ RGCs decreased (fig. S3). This suggests that the fraction of RGCs leaving the cell cycle at early stages of corticogenesis is lower for Cux2$^+$ RGCs than for Cux2$^-$ progenitors. To test this hypothesis, we analyzed cell cycle exit in *Cux2-Cre;Ai9* mice using a bromodeoxyuridine (BrdU) pulse to label S-phase cells at E12.5, followed by Ki67 staining at E13.5 to label cells that remained in the cell cycle (Fig. 3A). As expected, the fraction of Cux2$^+$ progenitors exiting the cell cycle was less than 50% that of Cux2$^-$ progenitors (Fig. 3B).

Because environmental cues such as notch-delta signaling control RGC self-renewal (*17*, *18*), we hypothesized that notch signaling may be preferentially active in Cux2$^+$ RGCs. However, notch signaling was not differentially regulated in Cux2$^+$ versus Cux2$^-$ RGCs (fig. S4, A to D), and activation of the pathway affected the two populations similarly (fig. S4, E to G). Rather, the proliferative behaviors of the two RGC subtypes

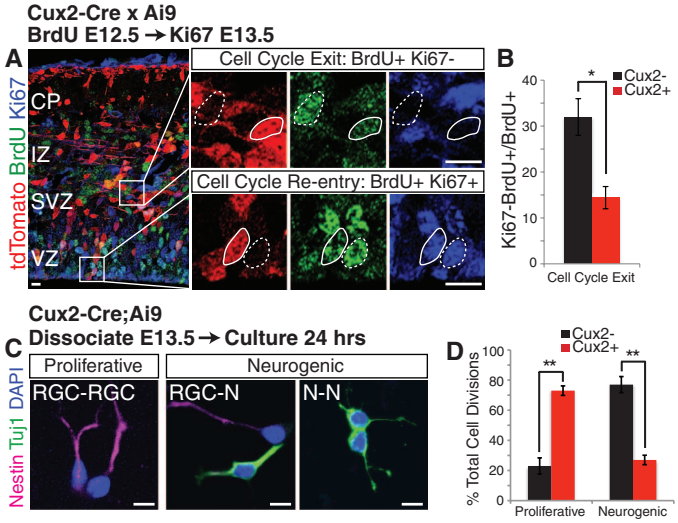

Fig. 3. During early neurogenesis, Cux2$^+$ progenitors are mainly proliferative, whereas Cux2$^-$ progenitors are neurogenic. (**A**) *Cux2-Cre;Ai9* embryos injected with BrdU to label S-phase cells at E12.5, then immunostained at E13.5 for BrdU and the proliferation marker Ki67. High magnifications of boxed areas at right show cells that exit (BrdU$^+$Ki67$^-$) or reenter (BrdU$^+$Ki67$^+$) the cell cycle within 24 hours. tdTomato absence (dotted outline) and presence (solid outline) identifies Cux2$^-$ and Cux2$^+$ cells, respectively. IZ, intermediate zone. (**B**) Percentage (±SEM) of Cux2$^-$ versus Cux2$^+$ progenitors that exit the cell cycle (BrdU$^+$Ki67$^-$). *P < 0.01. (**C**) Cortical cells from E13.5 *Cux2-Cre;Ai9* embryos cultured at single-cell density for 24 hours. Pairs of two nestin$^+$ RGCs indicate proliferative divisions; neurogenic divisions produce one or two Tuj1$^+$ neurons. Cux2$^-$ and Cux2$^+$ cells were identified by absence/presence of tdTomato (not shown). (**D**) Percentage (±SEM) of proliferative and neurogenic divisions in Cux2$^-$ versus Cux2$^+$ cell pairs. **P < 0.000001. Scale bars, 10 μm.

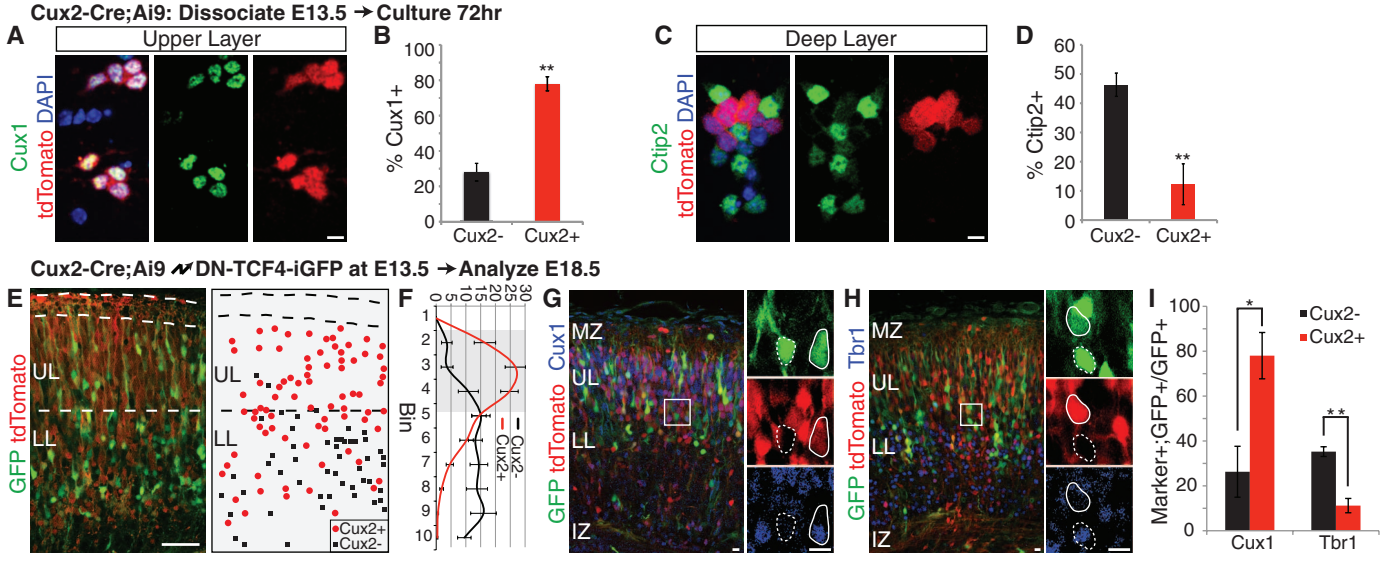

Fig. 4. Cux2$^+$ progenitors are intrinsically specified to generate upper-layer neurons, independently of niche or birthdate. (**A** to **D**) E13.5 *Cux2-Cre;Ai9* cortical cells cultured in vitro for 72 hours and stained for Cux1 (A) or Ctip2 (C). tdTomato absence/presence identified Cux2$^-$/Cux2$^+$ cells. Quantification is percentage (±SEM) of Cux2$^-$ versus Cux2$^+$ cells expressing Cux1 (B) or Ctip2 (D). **P < 0.0001. Scale bars, 10 μm. (**E** to **I**) *Cux2-Cre;Ai9* embryos electroporated at E13.5, analyzed at E18.5 for laminar position and molecular identity. (E) Example image shown on left; example schematic representation on right. UL, upper layers; LL, lower layers. Scale bar, 50 μm. (F) Cell position quantified by dividing the cortical plate into 10 equal-size bins. Graph shows percentage (±SEM) of electroporated Cux2$^-$ versus Cux2$^+$ cells in each bin. Upper-layer bins are shaded. (G and H) Immunostaining for Cux1 (G) and Tbr1 (H). High magnifications of boxed areas shown at right. tdTomato absence (dotted outline) and presence (solid outline) identified Cux2$^-$ and Cux2$^+$ cells, respectively. Scale bars, 10 μm. (I) Percentage (±SEM) of Cux2$^-$ versus Cux2$^+$ cells expressing Cux1 or Tbr1. *P < 0.02; **P < 0.005.

appear to be at least partially intrinsic, because these differences were maintained outside their normal niche. When cells from E13.5 *Cux2-Cre;Ai9* embryos were cultured in vitro at clonal density (Fig. 3C), the majority of $Cux2^+$ progenitors divided symmetrically to generate pairs of RGCs, whereas $Cux2^-$ progenitors preferentially underwent neurogenic divisions (Fig. 3D). We conclude that at early stages of corticogenesis, $Cux2^+$ RGCs fated to generate upper-layer neurons preferentially proliferate to enlarge the precursor pool, whereas $Cux2^-$ RGCs already generate lower-layer neurons.

We next asked whether the generation of distinct neuronal subtypes is an intrinsic property of the two different progenitor types. Dissociated cortical cells from *Cux2-Cre;Ai9* embryos were cultured until they differentiated and were stained with layer-specific markers (Fig. 4, A and C). The in vivo situation was recapitulated in vitro, with ~80% of the $Cux2^+$ progenitors generating neurons with upper-layer identity (Fig. 4B) and the majority of the $Cux2^-$ progenitors producing neurons with lower-layer identity (Fig. 4D). Thus, the neurogenic differences between the two progenitor populations are maintained outside their normal developmental niche, indicating an intrinsic aspect to their divergent fate specification. This result also suggests that birthdate may not be causative to cell fate. To test this hypothesis, we electroporated dominant-negative TCF4 into $Cux2^+$ RGCs to force their premature cell cycle exit (*19*), so that they generated neurons at the expense of self-renewal (fig. S5). These prematurely generated $Cux2^+$ neurons still preferentially occupied upper layers (Fig. 4, E and F) and expressed upper-layer, but not lower-layer, markers (Fig. 4, G to I), indicating that their fate was not altered by the change in birthdate. Thus, $Cux2^+$ RGCs are intrinsically specified to generate upper-layer neurons, independent of niche or birthdate.

Our data show that a subset of RGCs is specified to generate upper-layer neurons regardless of birthdate, but these progenitors are intrinsically programmed to generate neurons predominantly later than their lower-layer counterparts. Thus, contrary to the prevailing model (*2*), our study indicates that molecular fate specification ensures proper birth order, rather than vice versa. Our data also suggest that the minor fraction of callosal projection neurons found in lower layers is derived from the same RGC pool as the major population of callosal neurons in upper layers, demonstrating a common lineage for these functionally similar neurons, irrespective of cortical layer position. Although this model applies to the broad RGC subclasses that generate intracortical versus subcortical/subcerebral projection neurons, it remains possible that the potential of $Cux2^+$ and $Cux2^-$ progenitors is subsequently progressively restricted to further specify neuronal subtypes within the two lineages.

Upper cortical layers are expanded in primates and are required for high-level associative connectivity. Defects in their function are implicated in the etiology of cognitive syndromes such as schizophrenia and autism. The subventricular zone of primates, and especially humans, is enlarged compared with other species and contains outer subventricular RGCs that are thought to generate increased numbers of upper-layer cortical neurons in the primate brain (*20*). Our findings suggest that an equally important evolutionary advance was the subdivision of labor among RGCs in the ventricular zone to generate lower- and upper-layer neurons.

References and Notes

1. B. J. Molyneaux, P. Arlotta, J. R. L. Menezes, J. D. Macklis, *Nat. Rev. Neurosci.* **8**, 427 (2007).
2. D. P. Leone, K. Srinivasan, B. Chen, E. Alcamo, S. K. McConnell, *Curr. Opin. Neurobiol.* **18**, 28 (2008).
3. R. F. Hevner *et al.*, *Dev. Neurosci.* **25**, 139 (2003).
4. T. Kowalczyk *et al.*, *Cereb. Cortex* **19**, 2439 (2009).
5. M. Nieto *et al.*, *J. Comp. Neurol.* **479**, 168 (2004).
6. C. Zimmer, M.-C. Tiveron, R. Bodmer, H. Cremer, *Cereb. Cortex* **14**, 1408 (2004).
7. S. J. Franco, I. Martinez-Garay, C. Gil-Sanz, S. R. Harkins-Perry, U. Müller, *Neuron* **69**, 482 (2011).
8. E. A. Alcamo *et al.*, *Neuron* **57**, 364 (2008).
9. O. Britanova *et al.*, *Neuron* **57**, 378 (2008).
10. F. Schnütgen *et al.*, *Nat. Biotechnol.* **21**, 562 (2003).
11. R. Feil, J. Wagner, D. Metzger, P. Chambon, *Biochem. Biophys. Res. Commun.* **237**, 752 (1997).
12. S. Hayashi, A. P. McMahon, *Dev. Biol.* **244**, 305 (2002).
13. M. Zervas, S. Millet, S. Ahn, A. L. Joyner, *Neuron* **43**, 345 (2004).
14. F. Balordi, G. Fishell, *J. Neurosci.* **27**, 14248 (2007).
15. M. R. Costa, O. Bucholz, T. Schroeder, M. Götz, *Cereb. Cortex* **19** (suppl. 1), i135 (2009).
16. T. Takahashi, T. Goto, S. Miyama, R. S. Nowakowski, V. S. Caviness Jr., *J. Neurosci.* **19**, 10357 (1999).
17. K.-I. Mizutani, K. Yoon, L. Dang, A. Tokunaga, N. Gaiano, *Nature* **449**, 351 (2007).
18. K.-J. Yoon *et al.*, *Neuron* **58**, 519 (2008).
19. G. J. Woodhead, C. A. Mutch, E. C. Olson, A. Chenn, *J. Neurosci.* **26**, 12620 (2006).
20. J. H. Lui, D. V. Hansen, A. R. Kriegstein, *Cell* **146**, 18 (2011).

Acknowledgments: We thank G. Fishell for *Nestin-CreERT2* mice; H. Zeng for *Ai9* reporter mice; P. Chambon for *pCreERT2*; A. Maximov for the FLEx backbone; T. Wagner, S. Courtes, and P. Kazmierczak for experiments that did not appear in the final manuscript; and F. Polleux, E. Grove, N. Grillet, and S. Courtes for critical comments. This work was supported by the NIH (S.J.F., NS060355; U.M., NS046456 and MH078833), Generalitat Valenciana (C.G.-S., APOSTD/2010/064), Ministerio de Educacion (C.G.-S., EX2009-0416; I.M.-G., FU-2006-1238), CIRM training grant (I.M.-G. and A.E.), the Skaggs Institute for Chemical Biology (U.M.), and the Dorris Neuroscience Center (U.M.). S.J.F., I.M.-G., C.G.-S., and U.M. conceived the project; S.J.F., C.G.-S., I.M.-G., and A.E. designed, performed, and analyzed experiments with assistance from S.R.H.-P. and C.R.; and S.J.F. and U.M. prepared the manuscript, with revisions from C.G.-S., I.M.-G., and A.E.

Supplementary Materials

www.sciencemag.org/cgi/content/full/337/6095/746/DC1
Materials and Methods
Figs. S1 to S5
References (*21*–*29*)

20 April 2012; accepted 14 June 2012
10.1126/science.1223616

Bergmann Glial AMPA Receptors Are Required for Fine Motor Coordination

Aiman S. Saab,[1,2] Alexander Neumeyer,[3]* Hannah M. Jahn,[1,2]*† Alexander Cupido,[1]* Antonia A. M. Šimek,[4]* Henk-Jan Boele,[4] Anja Scheller,[1,2] Karim Le Meur,[1]‡ Magdalena Götz,[5,6] Hannah Monyer,[7] Rolf Sprengel,[8] Maria E. Rubio,[9] Joachim W. Deitmer,[3] Chris I. De Zeeuw,[4,10]§ Frank Kirchhoff[1,2]§

The impact of glial neurotransmitter receptors in vivo is still elusive. In the cerebellum, Bergmann glial (BG) cells express α-amino-3-hydroxy-5-methyl-4-isoxazolepropionic acid (AMPA)–type glutamate receptors (AMPARs) composed exclusively of GluA1 and/or GluA4 subunits. With the use of conditional gene inactivation, we found that the majority of cerebellar GluA1/A4-type AMPARs are expressed in BG cells. In young mice, deletion of BG AMPARs resulted in retraction of glial appendages from Purkinje cell (PC) synapses, increased amplitude and duration of evoked PC currents, and a delayed formation of glutamatergic synapses. In adult mice, AMPAR inactivation also caused retraction of glial processes. The physiological and structural changes were accompanied by behavioral impairments in fine motor coordination. Thus, BG AMPARs are essential to optimize synaptic integration and cerebellar output function throughout life.

Astroglial cells sense synaptic activity through various neurotransmitter receptors and are considered to modulate neuronal processing (*1*–*3*). In the cerebellar cortex, ectopic release of glutamate from climbing and parallel fiber terminals activates Ca^{2+}-permeable α-amino-3-hydroxy-5-methyl-4-isoxazolepropionic acid (AMPA)–type glutamate receptors (AMPARs) expressed on Bergmann glial (BG) appendages (*4*) that tightly enwrap Purkinje cell (PC) synapses (*5*). Conversion of BG AMPARs into Ca^{2+}-impermeable receptors by adenoviral-mediated delivery of the GluA2 gene (*6*) caused BG process retraction from PC synapses and altered PC excitatory postsynaptic currents (EPSCs), providing insight into the functional interaction between BG and glutamatergic synapses. However, whether BG AMPAR signaling influences cerebellar function in vivo has remained unknown.

Supplementary Materials for

Fate-Restricted Neural Progenitors in the Mammalian Cerebral Cortex

Santos J. Franco, Cristina Gil-Sanz, Isabel Martinez-Garay, Ana Espinosa,
Sarah R. Harkins-Perry, Cynthia Ramos, Ulrich Müller*

*To whom correspondence should be addressed. E-mail: umueller@scripps.edu

Published 10 August 2012, *Science* **337**, 746 (2012)
DOI: 10.1126/science.1223616

This PDF file includes:

Materials and Methods

Mice

Cux2-Cre (*7*), *Nestin-CreERT2* (*14*), *Rosa26* (*Gt(ROSA)26Sor*) (*21*), *Z/EG* (*Tg(ACTB-Bgeo/GFP)21Lbe*) (*22*), *Ai9* (*23*), *Brainbow* (*B6.Cg-Tg(Thy1-Brainbow1.0)HLich/J*) (*24*), and *FLPe* (B6.Cg-Tg(ACTFLPe)9205Dym/J) (*25*) mice have been previously described. *Brainbow* mice were crossed to *FLPe* mice for 4 generations to generate *Brainbow;FLPe*^{4}, which harbors only one copy of the Brainbow 1.0 transgene. *Cux2-CreERT2* mice were generated at inGenious Targeting Laboratory using an identical strategy as the *Cux2-Cre* strain (*7*), but using a modified *CreERT2* (*11*) gene with an engineered Kozak sequence. Tamoxifen induction of the *CreERT2* lines was performed by intraperitoneal injection of 2 mg tamoxifen (Sigma) dissolved in sunflower oil (Sigma) into pregnant mothers at the indicated times, except in some cases (Fig. 2, F and H; fig. S2, F and G) in which *Nestin-CreERT2* mice were induced with 0.02 mg tamoxifen to generate sparse labeling to facilitate quantification. Progesterone (Sigma) was co-administered at half the concentration of tamoxifen to prevent late abortions caused by the mixed-estrogen effects of tamoxifen. For postnatal analysis of tamoxifen-induced animals, pups were delivered by cesarean section at E19.5 and provided with a foster mother until analysis. Analysis was performed on 4 animals from 3 separate experiments for each condition.

In Situ Hybridization

In situ hybridization was carried out on 12 μm frozen sections as described (*26*). To generate the Cux2 sense and antisense probes, a 2.4kb fragment of the murine Cux2 gene was amplified from E15.5 mouse brain cDNA and cloned into pGEM-T (Promega) using the following primers: 5'-GCCCAGCGTGAGGTGGAAAG -3' and 5'-GGACCTCCTTGACTCTCTTGG -3'.

Immunohistochemistry

Immunostaining was performed as described (*7*). Sections used for BrdU immunostaining were first treated with 2N HCl for 20 minutes and washed twice with borate buffer pH 8.0 to equilibrate. Antibodies used for immunostaining were: anti-BrdU rat monoclonal (1:300; AbD Serotec), anti-Ki-67 mouse monoclonal (1:200; BD Pharmingen), anti-Ctip2 (25B6) rat monoclonal (1:500; Abcam), anti-Cux1 CDP (M-222) rabbit polyclonal (1:200; Santa Cruz Biotechnology), anti-FoxP2 rabbit polyclonal (1:500, Abcam), anti-GAD65/67 rabbit polyclonal (1:1000, Sigma), anti-nestin (Rat401) mouse monoclonal (1:10; Developmental Studies Hybridoma Bank, NICHD and University of Iowa Department of Biology), anti-Pax6 rabbit polyclonal (1:250, Covance), anti-Satb2 rabbit polyclonal (1:2000, Abcam), anti-Smi32 mouse monoclonal (1:2000, Abcam), anti-Tbr1 rabbit polyclonal (1:500; Abcam), anti-Tbr2 rabbit polyclonal (1:500; Abcam), anti-Tuj1 mouse monoclonal directly conjugated to Alexa-488 (1:2000, Covance), anti-βgal chicken polyclonal (1:2000; Abcam). Anti-RFP rabbit polyclonal (1:200, Abcam ab62341) was used to recover tdTomato signal only in sections treated with HCl. Nuclei were stained with ToPro3, YoYo1 or DAPI (1:5,000; Molecular Probes) and sections were mounted on slides with Prolong Gold mounting medium (Molecular Probes).

Cell Cycle Exit

BrdU was administered at E12.5 by IP injection at 100 mg/kg body weight into pregnant females resulting from *Cux2*$^{+/cre}$ x *Ai9*$^{+/fl}$ crosses. Embryos were dissected 24 hours after injection and brains were sectioned at 100 μm and processed for immunostaining for BrdU, Ki67 and tdTomato. For quantification of cell cycle exit, BrdU^{+} cells were first marked in a standardized cortical field from pia to ventricle. Next, BrdU^{+} cells were marked as either Ki67^{+} or Ki67^{-}. Finally, presence or absence of tdTomato signal was used to identify cells in the Cux2^{+} and Cux2^{-} lineage, respectively. Cell cycle exit was therefore quantified separately and blindly for Cux2^{+} and Cux2^{-} cells within the same sections, and shown as the percentage of BrdU^{+} cells that were Ki67- for each lineage. Analysis was performed on 4 animals from 3 separate experiments.

Expression Constructs

Control-iGFP (pCIG2) has been described (*27*). Dominant-negative TCF4 was amplified from E15.5 mouse brain cDNA using the primers 5'-ATCTCGAGTAAAATGAGCAGTGGGAAAAATGGACCAAC-3' (Bases 645 - 667 of NM_013685.2) and 5'-TCACATCTGTCCCATGTGATTCG-3' (Bases 2545 - 2567 of NM_013685.2) and cloned into pCIG2 to generate DN-TCF4-iGFP. Constitutively-active notch (notch intracellular domain) was amplified from pCAGGS-NICD (Addgene plasmid 26891) using primers 5'- CCTGAATTCGACCATGGACTACAAAG-3' and 5'-GTAGAATTCTTATTTAAATGCCTCTGGAATGTG-3' and cloned into pCIG2 to generate CA-notch-iGFP. Notch activity reporter constructs have been described (*17*). CBFRE-GFP (Addgene plasmid 17705) was used as is. Hes5p-GFP was generated by replacing dsRed2 with eGFP in Hes5p-dsRed (Addgene plasmid 26868). CβA-FLEx comprises: chicken β-actin promoter/intron (forward orientation), lox2372 (forward orientation), tdTomato (forward orientation), lox511 (forward orientation), GFP (reverse orientation), lox2372 (reverse orientation), lox511 (reverse orientation), and an SV40 polyA signal (forward orientation).

In Utero Electroporation

Timed pregnant mice were anesthetized and their uterine horns exposed. Endotoxin-free plasmid DNA (1-2 mg ml^{-1}) was injected into the embryos' lateral ventricles. For electroporation, 5 pulses separated by 900 ms were applied at 38 V for E12.5 embryos and at 40 V for E13.5 embryos. Embryos were allowed to develop *in utero* for the indicated time. For analysis of embryos, brains were fixed in 4% paraformaldehyde (PFA) overnight at 4°C. For postnatal analysis, pups were fixed by transcardial perfusion with 4% PFA before dissection and post-fixation. Brains were sectioned coronally at 100 μm with a vibrating microtome (VT1200S; Leica). Electroporations were analyzed from 3 animals from 3 separate experiments for each condition.

In Vitro Cultures of Primary Cortical Cells

Cerebral cortices of *Cux2-Cre;Ai9* embryos were dissected and dissociated with trypsin at E13.5. Single cell suspensions were plated on LabTek II 1.5 borosilicate coverglass chambers (Thermo Scientific/Nunc) coated with Matrigel basement membrane matrix (1:100, BD Biosciences). Cells were cultured 24 or 72 hours in serum-free

medium (*28*) without additional growth factors. For 24-hour cultures, live cells were imaged using an inverted brightfield microscope 1 hour and 24 hours after plating to identify single cells that divided once to generate cell pairs. Analysis was performed on 9 brains from 4 separate experiments per time point.

Slice Culture and Time-Lapse Imaging

Cux2$^{+/cre}$*;Ai9*$^{+/fl}$ embryos were dissected and brains processed for organotypic slice culture as described (*29*). Time-lapse imaging was performed using a 40x long-working distance objective on a Nikon A1R confocal laser microscope system with a temperature-controlled culture chamber containing 40% O_2 and 5% CO_2. An image z-stack ranging 10 μm in 2.5 μm steps was projected into a maximum intensity composite. Stacks were captured every 15 minutes. Image analysis was performed using Nikon NIS-Elements and Adobe Photoshop.

Statistics

Statistical analysis was performed using unpaired homoscedastic two-sample t-test, except for notch pathway experiments in Fig. S4. For notch pathway experiments, independence of the two variables, being electroporated (GFP$^+$) and being Cux2$^+$ (tdTomato$^+$), was determined for each construct. Each cell in a standardized field was counted as either red or not red (tdTomato±) and green or not green (GFP±) to calculate the expected and observed probabilities that a cell would be red given that it is green ([P(R|G)exp] and [P(R|G)obs], respectively). Averaged values from 3 separate experiments for each of the 4 red/green states were input into 2x2 contingency tables and Fisher's exact test was used to calculate the statistical significance (1-tailed p-value) of the contingency between GFP expression and tdTomato expression for each construct.

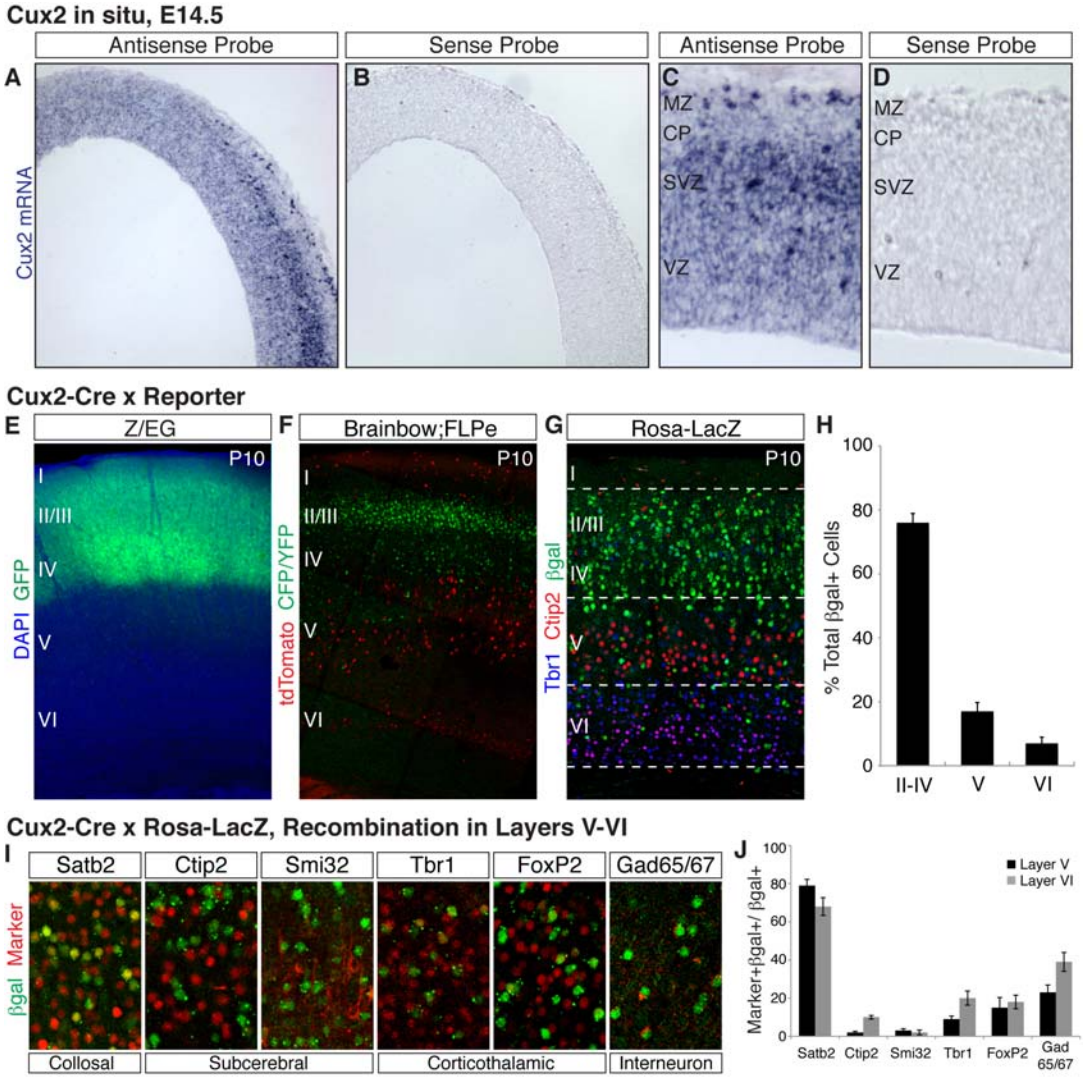

Fig. S1.

Related to Figure 1. (**A** and **B**) In situ hybridization of Cux2mRNA at E14.5 using antisense and sense probes. Note high expression in the marginal and subventricular zones and weaker expression in the cortical plate and ventricular zone. (**C** and **D**) Higher magnification images from examples in (A) and (B), respectively. (**E**-**H**) *Cux2-Cre* drives recombination of multiple reporter lines primarily in upper layer neurons at P10. (**E**) *Cux2-Cre* x *Z/EG* reporter. Recombined cells express GFP. (**F**) *Cux2-Cre* x *Brainbow;FLPe*[4]. Recombined cells express CFP or YFP, non-recombined cells express tdTomato. (**G**) *Cux2-Cre* x *Rosa-LacZ* reporter. Stained for markers of recombined cells (βgal), layer V neurons (Ctip2) and layer VI neurons (Tbr1). (**H**) Percentage of total βgal positive cells in each layer, ± SEM. (**I**) Characterization of recombined cells in lower layers V-VI in *Cux2-Cre*;*Rosa-LacZ* mice at P10. Stained for βgal and markers of callosal projection neurons (Satb2), subcerebral projection neurons (Ctip2, Smi32), corticothalamic projection neurons (Tbr1, FoxP2) and interneurons (Gad65/67). (**J**) Percentage of βgal^+ cells in layer V or VI that express each marker, ± SEM.

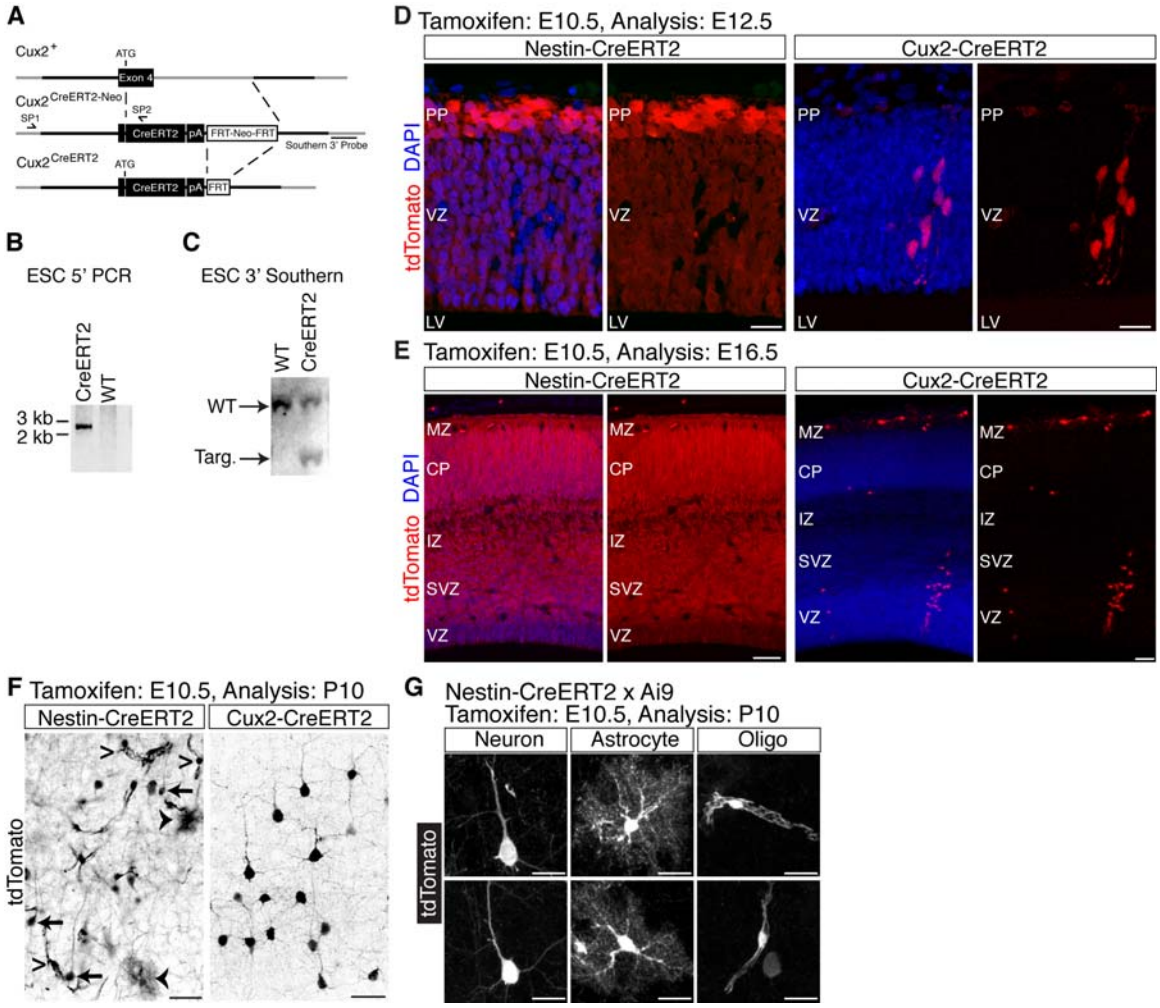

Fig. S2.

Related to Figure 2. (**A**) Targeting strategy for *Cux2-CreERT2* mice. SP1 and SP2, screening primers. (**B**) PCR analysis of 5' arm targeting using SP1 and SP2 in embryonic stem cells (ESC). (**C**) Southern blot for 3' arm targeting in ESCs. (**D** and **E**) CreERT2 mice were crossed to *Ai9* reporter mice. Pregnant females were injected with tamoxifen (2 mg) at E10.5. (**D**) *Nestin-CreERT2* mice drive recombination in nearly all RGCs at E12.5, including progenitors of preplate neurons. *Cux2-CreERT2* mice recombine in only a subset of RGCs, which are often found in clonal columns. (**E**) By E16.5, recombined cells in *Nestin-CreERT2;Ai9* mice include nearly all RGCs, intermediate progenitors, and their neuronal offspring in the cortical plate. Recombined cells in *Cux2-CreERT2* animals are mostly found in sparse clonal columns in the ventricular and subventricular zones, with very few recombined neurons. Scale bars, 10 μm (D) and 50 μm (E). (**F** and **G**) Tamoxifen induction at E10.5, analysis at P10. *Nestin-CreERT2* mice received 100-fold less tamoxifen than *Cux2-CreERT2* mice to facilitate visualization of single cells. (**F**) Recombination in *Nestin-CreERT2* brains is found in neurons (arrows), astrocytes (solid arrowheads) and oligodendrocytes (open arrowheads), whereas only neurons are labeled in *Cux2-CreERT2* brains. Scale bars, 50 μm. (**G**) Higher magnification of the various cell types labeled in *Nestin-CreERT2* mice. Scale bars, 10 μm.

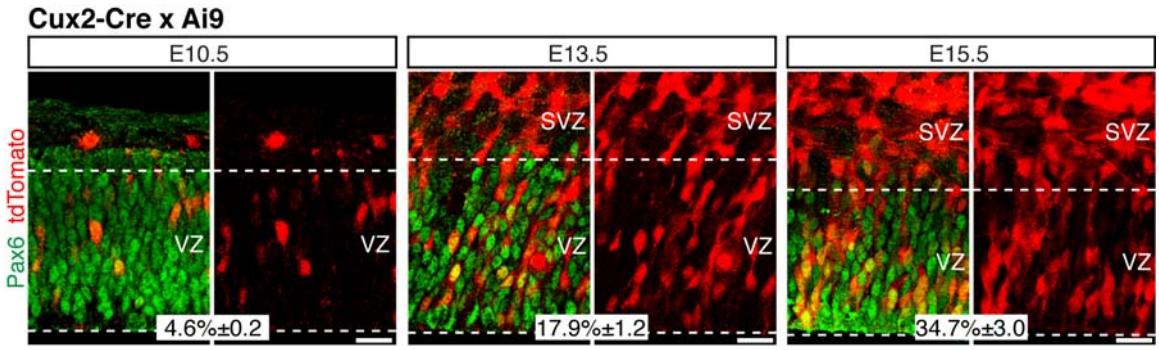

Fig. S3.

Related to Figure 3. Pax6 immunostaining in *Cux2-Cre;Ai9* embryos at E10.5, E13.5 and E15.5 demonstrates that the percentage of $Cux2^{+}$ RGCs increases over time. Percentage of $Pax6^{+}$ cells that are $tdTomato^{+}$ for each timepoint is indicated at the bottom of each set of images.

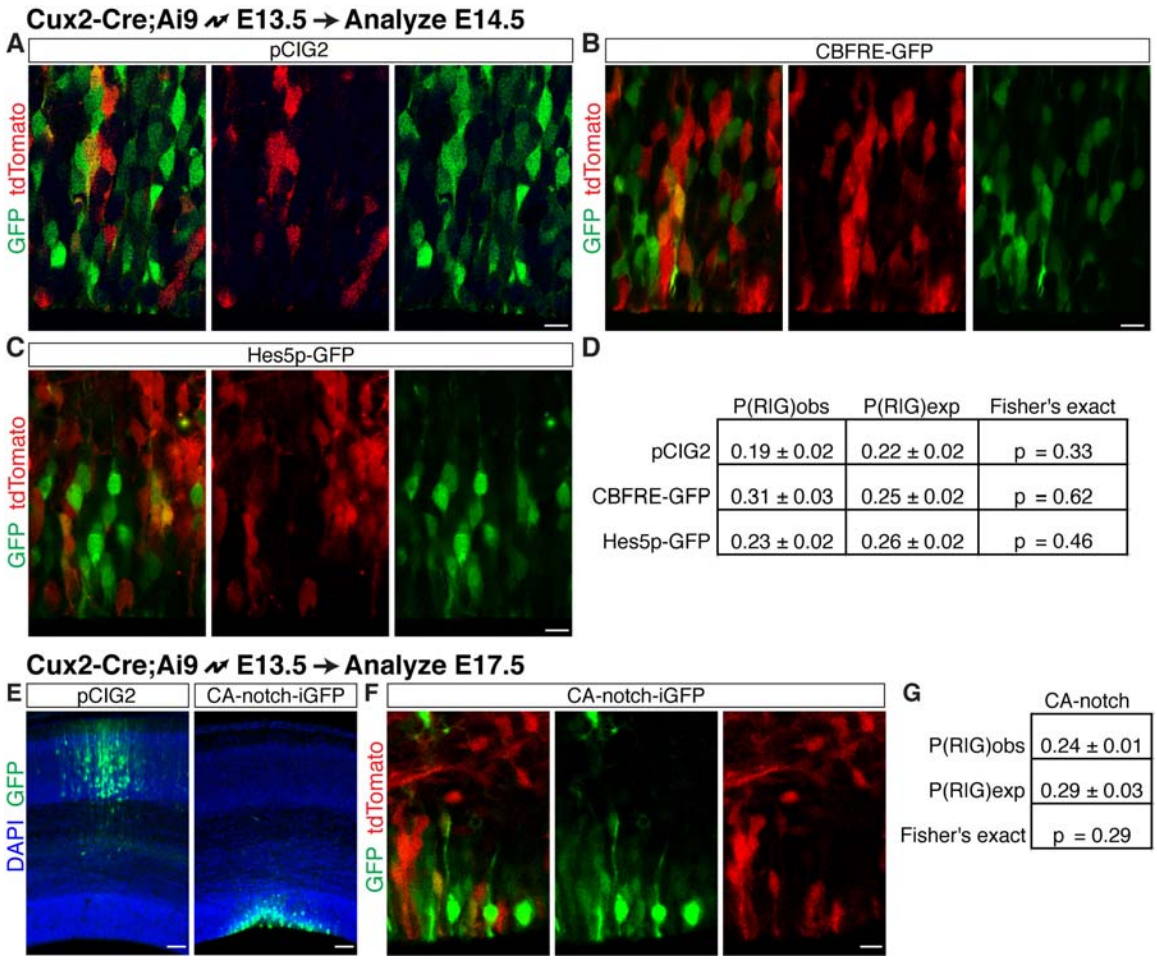

Fig. S4.

Related to Figure 3. (**A-D**) Notch-activity reporters are not preferentially active in Cux2$^+$ or Cux2$^-$ RGCs. *Cux2-Cre;Ai9* embryos electroporated at E13.5 with: (**A**) control pCIG2 vector, which expresses GFP ubiquitously from the chicken β-actin promoter; (**B**) notch activity reporter plasmid CBFRE-GFP, which expresses GFP from the CBF1 responsive element; (**C**) notch activity reporter plasmid Hes5p-GFP, which expresses GFP from the Hes5 promoter. Analysis at E14.5. Scale bars, 10 μm. (**D**) Quantification of tdTomato expression in electroporated GFP$^+$ cells, as described in Materials and Methods. Shown for each construct are the expected and observed probabilities that a cell would be red given that it is green ([P(R|G)exp] and [P(R|G)obs], respectively), ± SEM, and the 1-tailed p-value (by Fisher's exact test) of the contingency between expression of GFP and tdTomato. (**E-G**) Overexpression of constitutively active notch maintains the RGC state, but does not alter subtype identity. *Cux2-Cre;Ai9* embryos electroporated at E13.5, analyzed at E17.5. (**E**) Representative images of electroporations with control pCIG2 or CA-notch-iGFP, illustrating that CA-notch prevents neurogenesis and maintains cells in the RGC state. Scale bar 50 μm. (**F**) Representative images of CA-notch-iGFP electroporations demonstrating both Cux2$^+$ and Cux2$^-$ RGCs amongst the electroporated cells, indicating that CA-notch did not alter RGC subtype fate. Scale bar 10 μm. (**G**) Quantification of tdTomato expression in CA-notch-iGFP cells, as in (D).

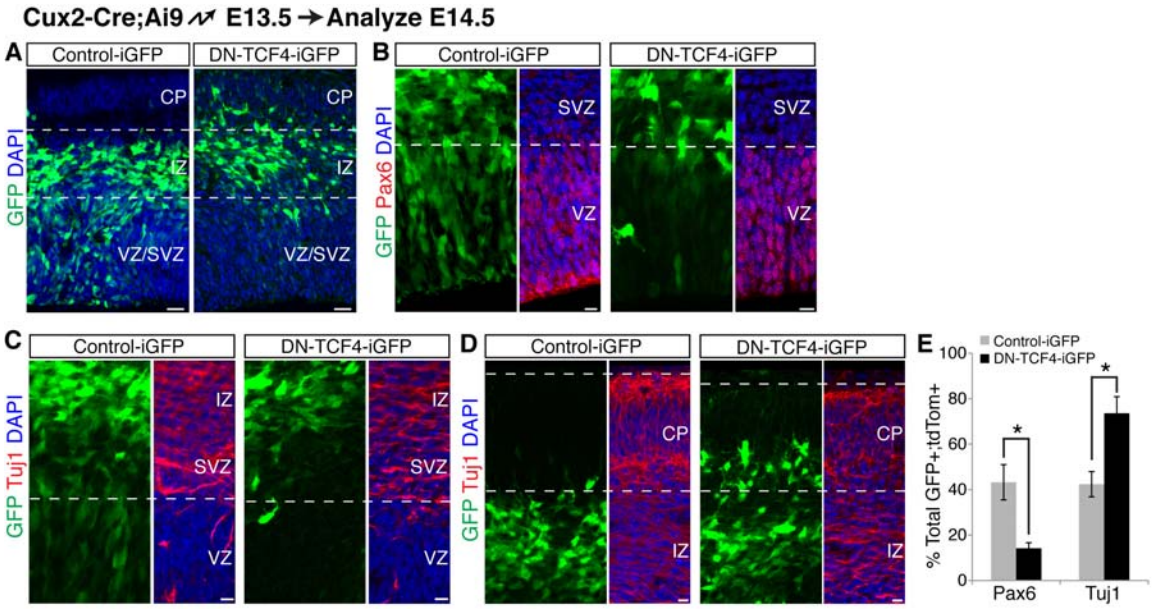

Fig. S5.

Related to Figure 4. (**A**-**E**) Interfering with β-catenin signaling forces premature differentiation of Cux2$^+$ RGCs in vivo. *Cux2-Cre;Ai9* embryos were electroporated in utero at E13.5 with control IRES-GFP or dominant-negative TCF4-IRES-GFP to block β-catenin signaling. (**A**) At E14.5, control cells are located in the ventricular, subventricular and intermediate zones, whereas most cells expressing DN-TCF4 have left the ventricular and subventricular zones and are already found entering the cortical plate. (**B**) Fewer DN-TCF4 expressing cells are in the Pax6$^+$ ventricular zone, compared to controls. (**C** and **D**) More DN-TCF4 expressing cells are in the Tuj1$^+$ subventricular and intermediate zones (C) and cortical plate (D), compared to controls. Scale bars, 25 μm. (**E**) Quantification of Pax6 and Tuj1 expression in the electroporated Cux2$^+$ (GFP$^+$, tdTomato$^+$) population. *, $P < 0.03$.

References

1. B. J. Molyneaux, P. Arlotta, J. R. L. Menezes, J. D. Macklis, Neuronal subtype specification in the cerebral cortex. *Nat. Rev. Neurosci.* **8**, 427 (2007). doi:10.1038/nrn2151 Medline

2. D. P. Leone, K. Srinivasan, B. Chen, E. Alcamo, S. K. McConnell, The determination of projection neuron identity in the developing cerebral cortex. *Curr. Opin. Neurobiol.* **18**, 28 (2008). doi:10.1016/j.conb.2008.05.006 Medline

3. R. F. Hevner *et al*., Beyond laminar fate: toward a molecular classification of cortical projection/pyramidal neurons. *Dev. Neurosci.* **25**, 139 (2003). doi:10.1159/000072263 Medline

4. T. Kowalczyk *et al*., Intermediate neuronal progenitors (basal progenitors) produce pyramidal-projection neurons for all layers of cerebral cortex. *Cereb. Cortex* **19**, 2439 (2009). doi:10.1093/cercor/bhn260 Medline

5. M. Nieto *et al*., Expression of Cux-1 and Cux-2 in the subventricular zone and upper layers II-IV of the cerebral cortex. *J. Comp. Neurol.* **479**, 168 (2004). doi:10.1002/cne.20322 Medline

6. C. Zimmer, M.-C. Tiveron, R. Bodmer, H. Cremer, Dynamics of Cux2 expression suggests that an early pool of SVZ precursors is fated to become upper cortical layer neurons. *Cereb. Cortex* **14**, 1408 (2004). doi:10.1093/cercor/bhh102 Medline

7. S. J. Franco, I. Martinez-Garay, C. Gil-Sanz, S. R. Harkins-Perry, U. Müller, Reelin regulates cadherin function via Dab1/Rap1 to control neuronal migration and lamination in the neocortex. *Neuron* **69**, 482 (2011). doi:10.1016/j.neuron.2011.01.003 Medline

8. E. A. Alcamo *et al*., Satb2 regulates callosal projection neuron identity in the developing cerebral cortex. *Neuron* **57**, 364 (2008). doi:10.1016/j.neuron.2007.12.012 Medline

9. O. Britanova *et al*., Satb2 is a postmitotic determinant for upper-layer neuron specification in the neocortex. *Neuron* **57**, 378 (2008). doi:10.1016/j.neuron.2007.12.028 Medline

10. F. Schnütgen *et al*., A directional strategy for monitoring Cre-mediated recombination at the cellular level in the mouse. *Nat. Biotechnol.* **21**, 562 (2003). doi:10.1038/nbt811 Medline

11. R. Feil, J. Wagner, D. Metzger, P. Chambon, Regulation of Cre recombinase activity by mutated estrogen receptor ligand-binding domains. *Biochem. Biophys. Res. Commun.* **237**, 752 (1997). doi:10.1006/bbrc.1997.7124 Medline

12. S. Hayashi, A. P. McMahon, Efficient recombination in diverse tissues by a tamoxifen-inducible form of Cre: a tool for temporally regulated gene activation/inactivation in the mouse. *Dev. Biol.* **244**, 305 (2002). doi:10.1006/dbio.2002.0597 Medline

13. M. Zervas, S. Millet, S. Ahn, A. L. Joyner, Cell behaviors and genetic lineages of the mesencephalon and rhombomere 1. *Neuron* **43**, 345 (2004). doi:10.1016/j.neuron.2004.07.010 Medline

14. F. Balordi, G. Fishell, Mosaic removal of hedgehog signaling in the adult SVZ reveals that the residual wild-type stem cells have a limited capacity for self-renewal. *J. Neurosci.* **27**, 14248 (2007). doi:10.1523/JNEUROSCI.4531-07.2007 Medline

15. M. R. Costa, O. Bucholz, T. Schroeder, M. Götz, Late origin of glia-restricted progenitors in the developing mouse cerebral cortex. *Cereb. Cortex* **19**, (Suppl 1), i135 (2009). doi:10.1093/cercor/bhp046 Medline

16. T. Takahashi, T. Goto, S. Miyama, R. S. Nowakowski, V. S. Caviness, Jr., Sequence of neuron origin and neocortical laminar fate: relation to cell cycle of origin in the developing murine cerebral wall. *J. Neurosci.* **19**, 10357 (1999). Medline

17. K.-I. Mizutani, K. Yoon, L. Dang, A. Tokunaga, N. Gaiano, Differential Notch signalling distinguishes neural stem cells from intermediate progenitors. *Nature* **449**, 351 (2007). doi:10.1038/nature06090 Medline

18. K.-J. Yoon *et al*., Mind bomb 1-expressing intermediate progenitors generate notch signaling to maintain radial glial cells. *Neuron* **58**, 519 (2008). doi:10.1016/j.neuron.2008.03.018 Medline

19. G. J. Woodhead, C. A. Mutch, E. C. Olson, A. Chenn, Cell-autonomous beta-catenin signaling regulates cortical precursor proliferation. *J. Neurosci.* **26**, 12620 (2006). doi:10.1523/JNEUROSCI.3180-06.2006 Medline

20. J. H. Lui, D. V. Hansen, A. R. Kriegstein, Development and evolution of the human neocortex. *Cell* **146**, 18 (2011). doi:10.1016/j.cell.2011.06.030 Medline

21. G. Friedrich, P. Soriano, Promoter traps in embryonic stem cells: a genetic screen to identify and mutate developmental genes in mice. *Genes Dev.* **5**, 1513 (1991). doi:10.1101/gad.5.9.1513 Medline

22. A. Novak, C. Guo, W. Yang, A. Nagy, C. G. Lobe, Z/EG, a double reporter mouse line that expresses enhanced green fluorescent protein upon Cre-mediated excision. *Genesis* **28**, 147 (2000). doi:10.1002/1526-968X(200011/12)28:3/4<147::AID-GENE90>3.0.CO;2-G Medline

23. L. Madisen *et al*., A robust and high-throughput Cre reporting and characterization system for the whole mouse brain. *Nat. Neurosci.* **13**, 133 (2010). doi:10.1038/nn.2467 Medline

24. J. Livet *et al*., Transgenic strategies for combinatorial expression of fluorescent proteins in the nervous system. *Nature* **450**, 56 (2007). doi:10.1038/nature06293 Medline

25. C. I. Rodríguez *et al*., High-efficiency deleter mice show that FLPe is an alternative to Cre-loxP. *Nat. Genet.* **25**, 139 (2000). doi:10.1038/75973 Medline

26. M. C. Tiveron, M. R. Hirsch, J. F. Brunet, The expression pattern of the transcription factor Phox2 delineates synaptic pathways of the autonomic nervous system. *J. Neurosci.* **16**, 7649 (1996). Medline

27. R. Hand *et al*., Phosphorylation of Neurogenin2 specifies the migration properties and the dendritic morphology of pyramidal neurons in the neocortex. *Neuron* **48**, 45 (2005). doi:10.1016/j.neuron.2005.08.032 Medline

28. X. Qian, S. K. Goderie, Q. Shen, J. H. Stern, S. Temple, Intrinsic programs of patterned cell lineages in isolated vertebrate CNS ventricular zone cells. *Development* **125**, 3143 (1998). Medline

29. F. Polleux, A. Ghosh, The slice overlay assay: a versatile tool to study the influence of extracellular signals on neuronal development. *Sci. STKE* **2002**, pl9 (2002). doi:10.1126/stke.2002.136.pl9 Medline